Hollow nanosystem-boosting synergistic effect between photothermal therapy and chemodynamic therapy via self-supplied hydrogen peroxide and relieved hypoxia

YunJi Sun[1,2]，Lixiao Zhen[1]，Lin Xu[1],Peipei Li[1]，Chao Zhang[2]，Yang Zhang[4]，YiSheng Zhao[3]，BenKang Shi[2]

1 Shandong Provincial Third Hospital,Shandong University, Jinan,Shandong,250031,P.R.China;

2 Qilu Hospital,Shandong University, Jinan,Shandong,250012,P.R.China;

3 School of Pharmaceutical Sciences, Key Laboratory for Natural Active Pharmaceutical Constituents Research in Universities of Shandong ProvinceShandong Analysis and Test Center, Qilu University of Technology (Shandong Academy of Sciences), Jinan, Shandong, 250353,P.R.China;

4 Shandong Provincial Hospital Affiliated to Shandong First Medical University, Jinan 250021, P.R.China;

*Correspondence:Benkang Shi:Qilu Hospital,107 Wenhua West Road, Lixia District, Jinan City, Shandong Province, China.
Email:shibenkangsdu@163.com； bkangshi@163.com; Yang zhang:Shandong Provincial Hospital Affiliated to Shandong First Medical University, Jinan 250021, P.R.China;Email: wonderfulwater1989@163.com; Yisheng Zhao :School of Pharmaceutical Sciences, Shandong Analysis and Test Center, Qilu University of Technology (Shandong Academy of Sciences), Jinan 250353, China.
Email:yisheng_zhao@qlu.edu.cn

Supplementary Figure Legends

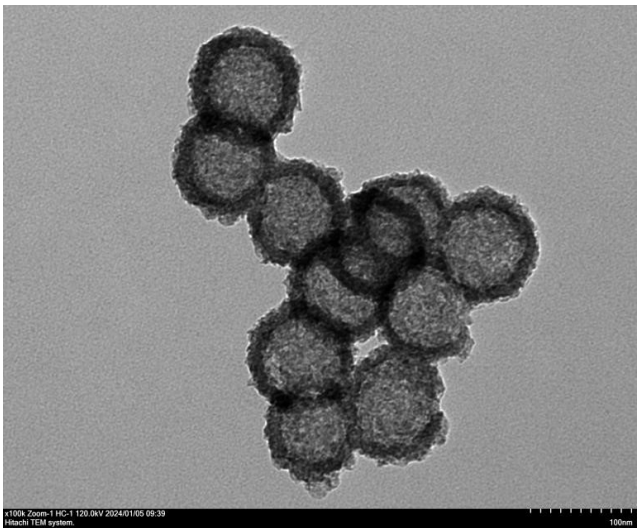

Figure S1. *TEM images：Nanoparticle composites exhibit excellent dispersion characteristics under high-magnification TEM.*

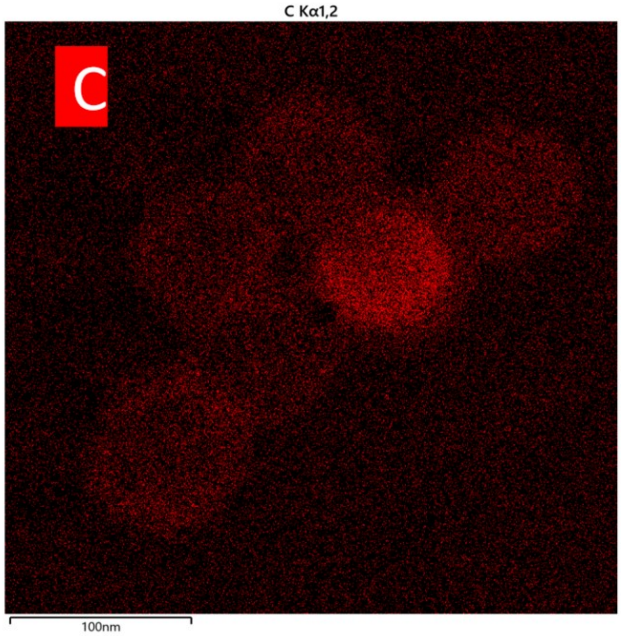

Figure S2*. TEM images：the distribution of carbon elements*

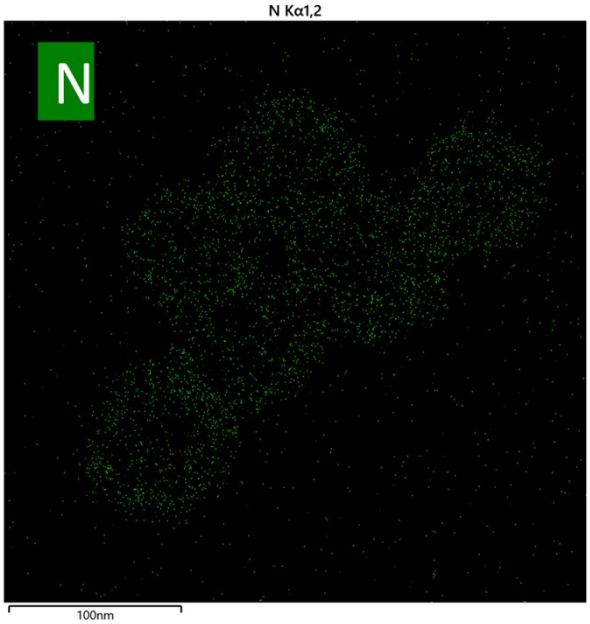

Figure S3. *TEM images the distribution of nitrogen elements*

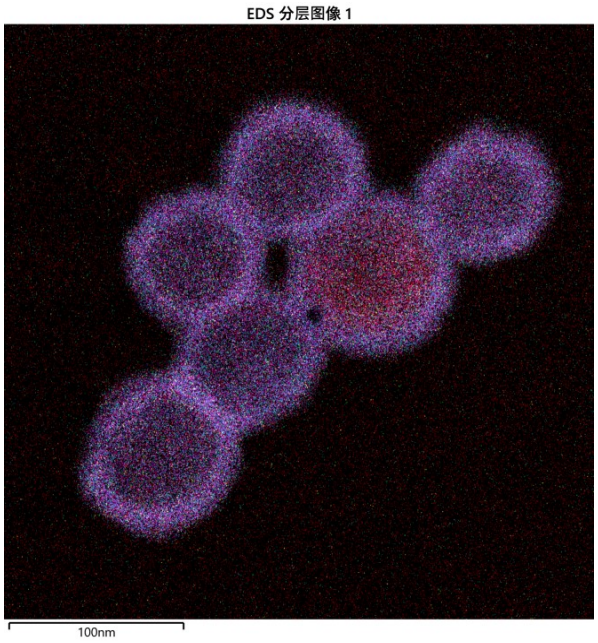

Figure S4. *TEM images： the distribution of nitrogen elements EDS*

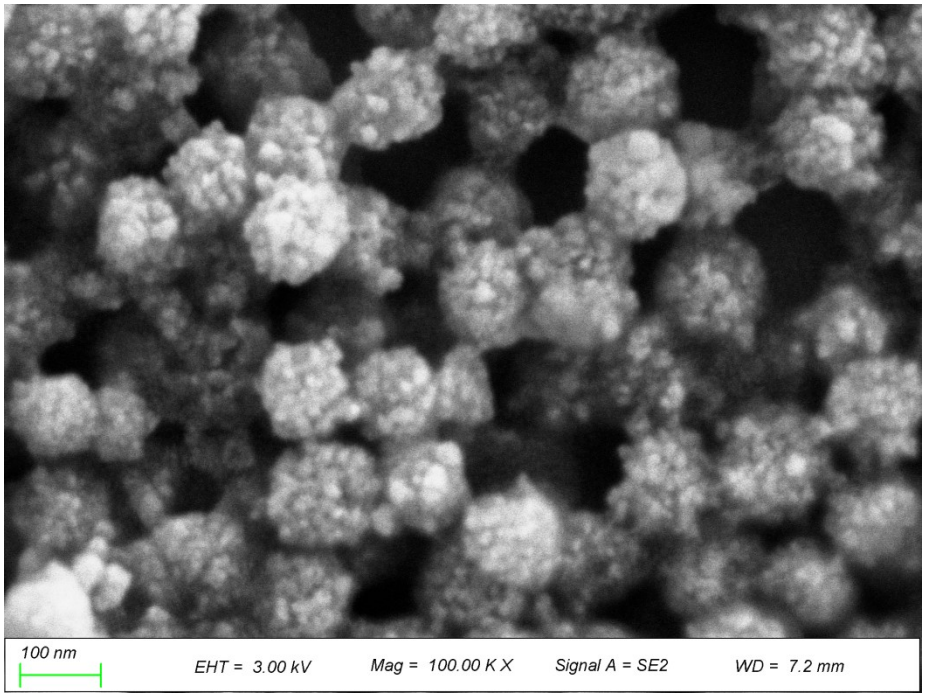

Figure S5. *SEM images： The nanocomposite particles exhibit uniform size distribution with peak sizes centered around 100 nm.*

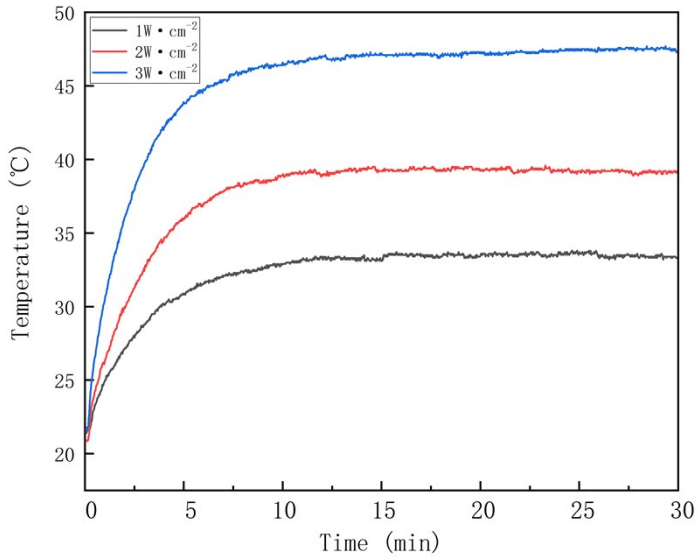

Figure S6. *Curves showing the time-course temperature variation of the H-MnO_2@IR825-VC solution upon irradiation at laser densities of 1, 2, and 3 W/cm^2.*

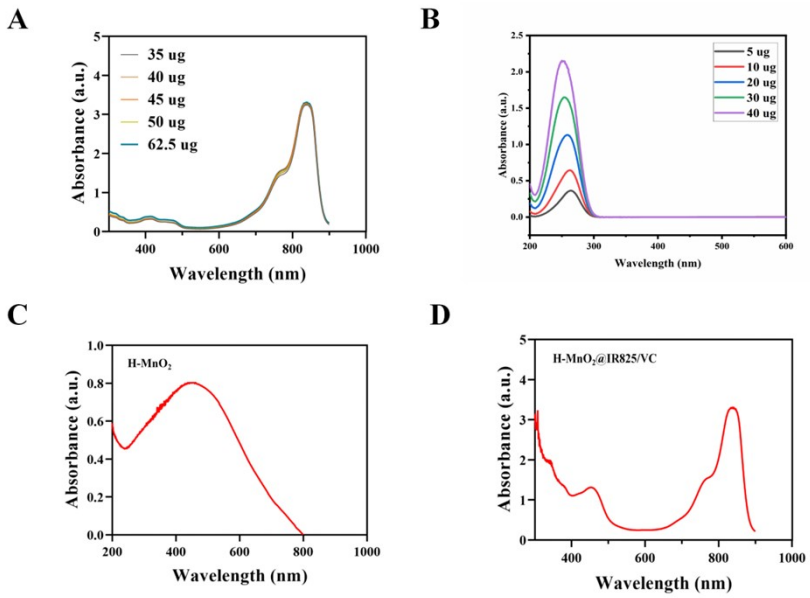

Figure S7. *The UV spectra of the particles. (A) The UV spectra of IR825 solution. (B) The UV spectra of VC solution. (C) The UV spectra of H-MnO_2 solution. (D) The UV spectra of H-MnO_2@IR825/VC solution.*

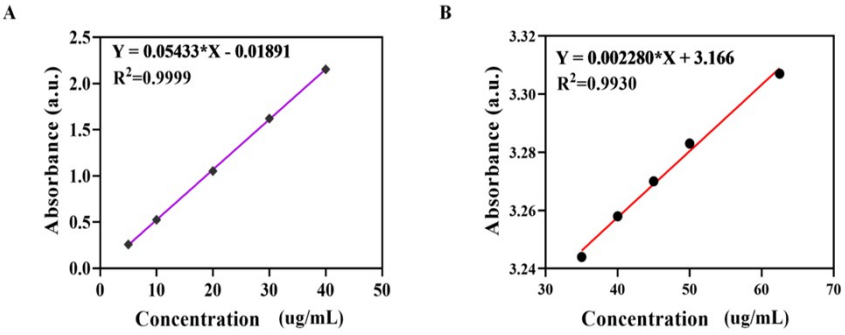

Figure S8. *A:The standard curve of absorbance values for VC solution;B:The standard curve of absorbance values for IR825 solution*

Comment []: The results showed that IR825 and VC were successfully loaded on H-MnO_2, and there was no mutual interference between them.

Comment []: The standard curves of VC solution and IR825 solution were established to calculate the drug loading.

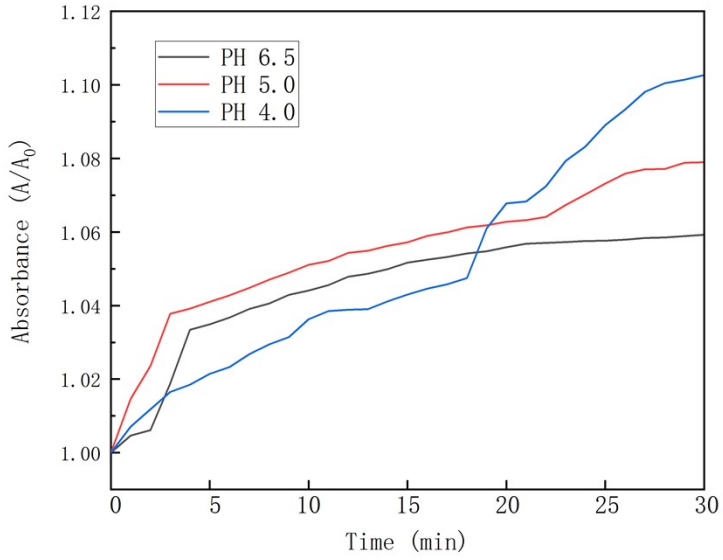

Figure S9. *The ability of the synthesized H-MnO_2@IR825-VC to generate hydroxyl radicals was investigated to explore the different reaction PH*

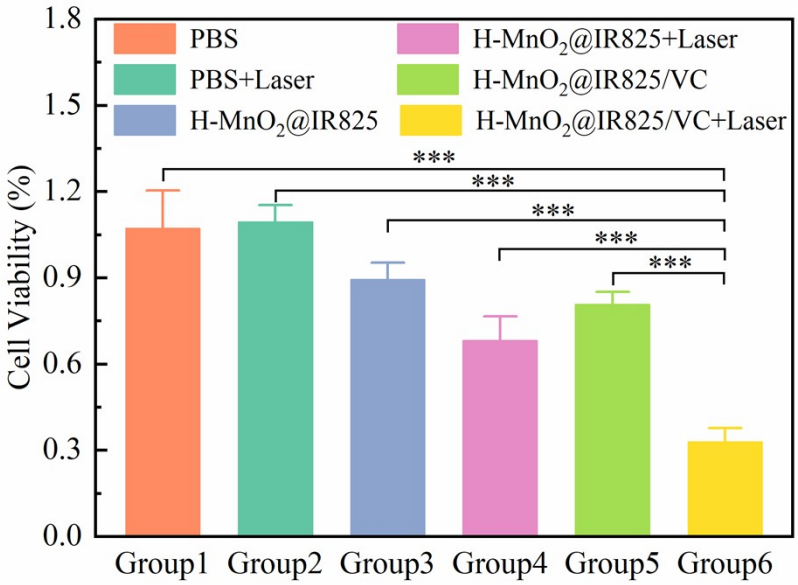

Figure S10. *Measurement of cell activity in each experimental group in hypoxic incubator.*

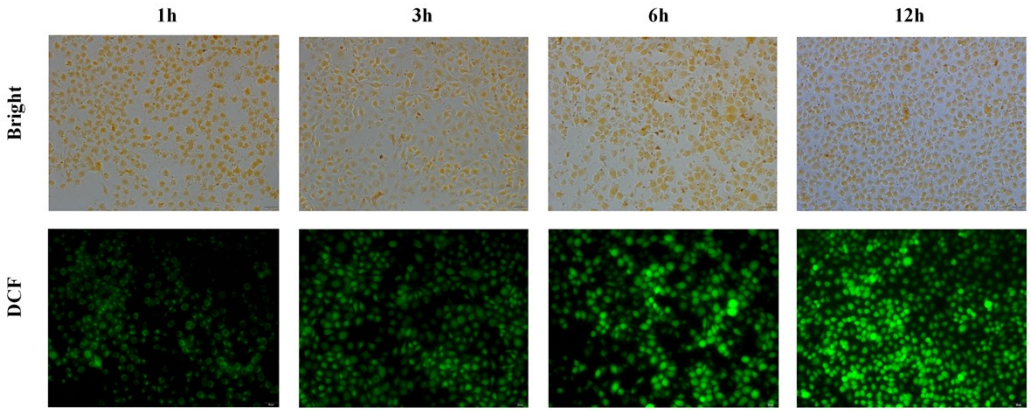

Figure S11.*Representative images showing the time-course phagocytosis of PC3 cells on FITC-labeled H-MnO_2@IR825-VC nanoparticles.*

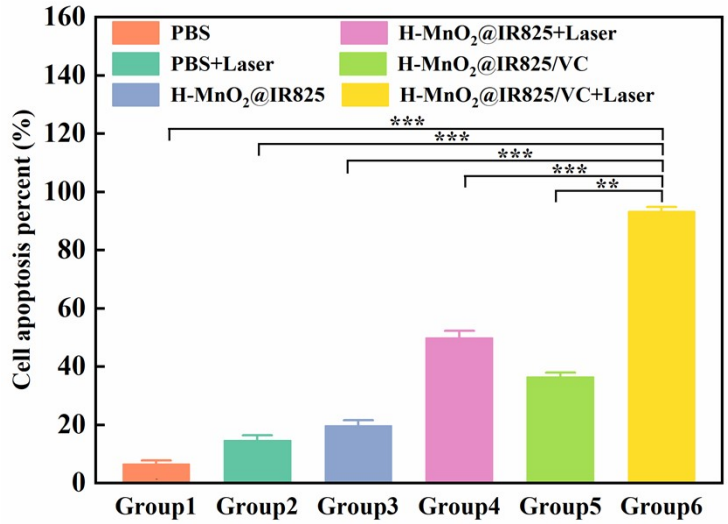

Figure S12.*Quantitative analysis of cell apoptosis was performed on PC3 cells from each experimental group after Annexin V/PI staining, followed by statistical analysis of the data obtained from flow cytometry.*

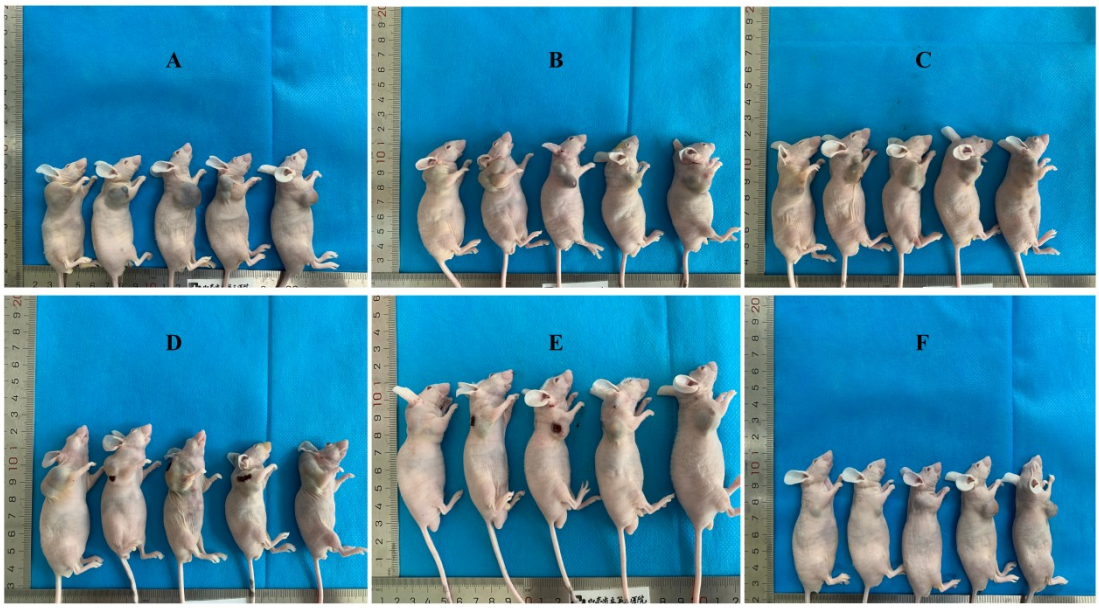

Figure S13.*Representative images of tumor-bearing nude mice treated with: A. PBS; B. H-MnO_2@IR825; C. H-MnO_2@IR825-VC; D. PBS+Laser; E. H-MnO_2@IR825+Laser; and F. H-MnO_2@IR825-VC+Laser.*

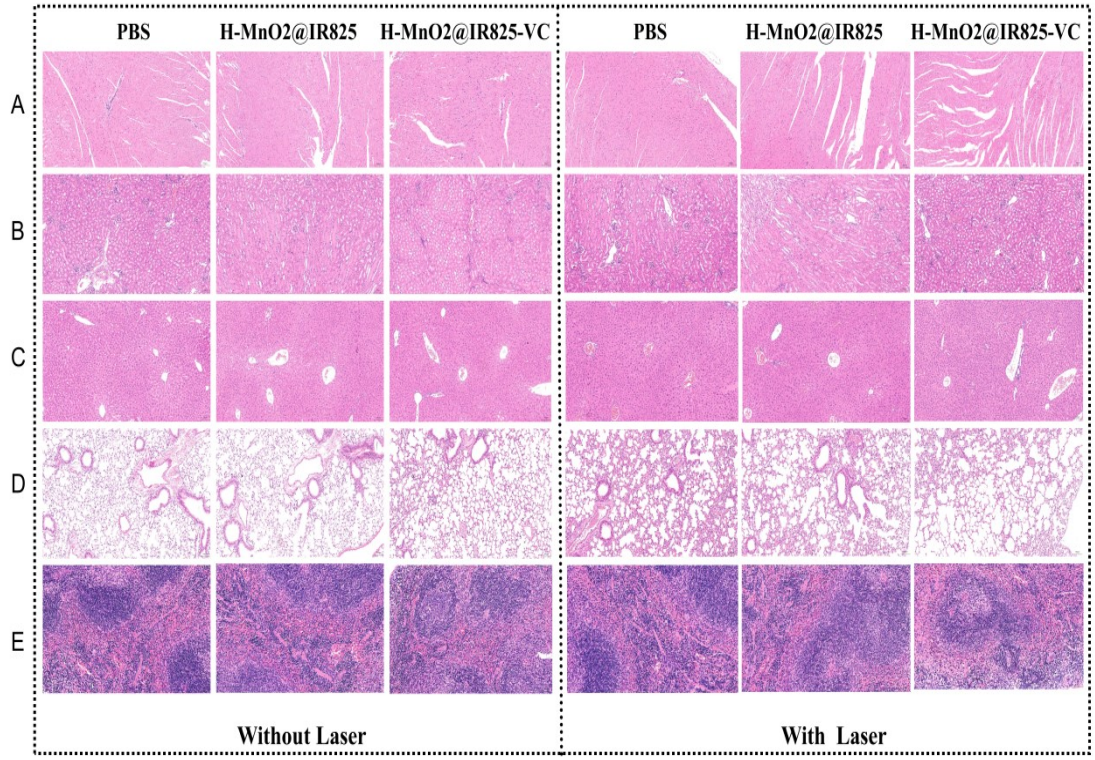

Figure S14. *Representative images of HE staining of organ section tissues of nude mice in each experimental group after treatment. A. Heart; B. Kidney; C. Liver; D. Lungs; E. Spleen.*